Title: **Sleep need driven oscillation of glutamatergic synaptic phenotype**

Kaspar Vogt[1], Ashwinikumar Kulkarni[2], Richa Pandey[3], Mantre Dehnad[3], Genevieve Konopka[2], Robert Greene[1,2,3,*]

1) International Institute of Integrative Sleep Medicine, University of Tsukuba, Tsukuba, Japan

2) Department of Neuroscience, Peter O'Donnell Brain Institute, University of Texas Southwestern Medical Center, Dallas, United States

3) Department of Psychiatry, Peter O'Donnell Brain Institute, University of Texas Southwestern Medical Center, Dallas, United States

*) Corresponding author

Abstract:

The response to sleep loss, induced by experimental sleep deprivation (SD), provides insight into the function of sleep. Earlier observations have shown an overall increase in synaptic strength and number of cortical, glutamate, AMPA receptor (AMPAR) synapses in response to SD that is recovered by sleep. However, other aspects of glutamatergic transmission, including NMDA receptor mediated neurotransmission and related upstream synaptic regulators of the glutamate synapse function, have not been well examined. Following SD, we report increased AMPA/NMDA ratio in whole cell recordings of frontal cortical (FC) pyramidal neurons of layers 2-3. Additionally, the ratio of silent/active synapse is decreased after SD reflecting decreased silent synapses and plastic potential to convert silent NMDA to active AMPA synapses. All aspects recover with sleep and are associated with differentially expressed genes (DEGs) affecting glutamatergic synaptic phenotype. The DEGs are enriched for a functional group of synaptic shaping cellular components (SSCs) controling glutamate synapse phenotype, overlap with autism risk genes and are primarily observed in a subtype of excitatory pyramidal neurons that project intra-telencephalically (ExIT neurons). Upstream, sleep-related control is suggested by significant enrichment of genes controlled by transcription factor, MEF2c and nuclear HDAC4, a repressor of MEF2c transcriptional activation. Taken together, we propose a functional role of sleep/wake in FC controlling gene expression, regulating an oscillation of glutamate-synaptic phenotypes that facilitates motor learning and training, and if dysfunctional, increases risk for autism.

Introduction

CNS control of arousal maintains waking neuronal activities needed for foraging, danger avoidance and reproductive behaviors. Reduction of arousal to unconsciousness can gate sleep, however, the function served by this sleep, in contrast to wake function, remains enigmatic. A reasonable teleologically oriented goal is more effective future foraging, danger avoidance and reproductive behaviors, based on learning from past waking experience. Effective learning involves memory of waking experience and underlying long-term plasticity[1-3](LTP). At the cellular level, extensive activity dependent LTP of cortical glutamate synapses can lead to a well-documented increase of synaptic strength of cortical glutamatergic synapses during waking. It is reflected by increased frequency and amplitude of glutamatergic miniature synaptic currents (mEPSC) that is restored by subsequent sleep[4, 5], consistent with the synaptic homeostasis hypothesis of sleep (SHY)[6].

Our recent findings indicate that during waking, not only are individual synapses strengthened (overall glutamate mEPSC amplitude in layer 2-3 pyramidal cells is increased by SD) but, also, the number of electro-physiologically active synapses is increased (increased frequency in correlation with unaltered or

decreased probability of release)[7]. The molecular underpinnings of these changes in glutamate synaptic strength and number were examined to determine the changes in the glutamate synaptic phenotype and what the implication(s) of these changes, if any, might be with regards to propensity for synaptic plasticity (meta-plasticity).

We investigated sleep/wake mediated electrophysiological changes in glutamatergic synapses in motor cortex, layer 2-3, pyramidal neurons since our previous work demonstrates wake/sleep up-regulation and down-regulation, respectively, in these cells' glutamate synapses[7]. We observed a wake/sleep oscillation of AMPA/NMDA synaptic response ratio in pyramidal neurons of motor neocortex coupled with an oscillating fraction of silent synapses (NMDAR-mediated synaptic response but no AMPAR mediated response) in response to sleep need. We then, extended these physiological findings to include characterization of sleep-need related differential expression of glutamatergic synaptic shaping genes that can control the observed oscillating glutamate synapse phenotype.

Results

Three cohorts of C57 BL/6 male mice were allowed either to 1) sleep ad lib (control sleep, CS); 2) prevented from sleeping from ZT=0 to 6h (sleep deprived, SD); or, 3) after 4h SD allowed recovery sleep, ad lib for 2h (RS). *Ex Vivo* acute brain slices from the motor cortex were then prepared from these animals at ZT=6h and whole cell recordings obtained from layer 2/3 pyramidal neurons (see methods for details). Locally evoked glutamatergic EPSCs recorded at -90mV had little NMDAR contribution due to Mg^{++} block. These were compared in the same cell, to EPSCs evoked at +50mV with little AMPAR contribution due to reduced AMPAR driving force, but, having large NMDAR currents due to voltage sensitive relief from Mg^{++} blockade (NMDAR currents had reversed polarity since E_{NMDAR} =~0mV). For each recorded neuron (one neuron/ slice/ animal) an average response to repeated stimuli (>10 stimuli applied every 10sec) to elicit a EPSC (~50% of maximal amplitude) was determined at each holding potential. A two-way ANOVA analysis showed a significant interaction between AMPA matched to NMDA EPSC response, and sleep condition ($F(2, 21) = 7.268$, $p<0.004$; Figure 1 A, C, E). When considered independently, neither the effect of sleep condition nor of EPSC subtype reached significance at $p<0.05$ (Figure 1 C).

To control for slice/subject EPSC variability from stimulation-evoked afferent variability, we calculated the AMPA/NMDA ratio, matched for each recorded neuron. This showed a significantly greater AMPA/NMDA EPSC ratio comparing SD to CS or RS when analyzed with Kruskal-Wallis test and two-stage linear step-up procedure of Benjamini, Krieger, Yekutieli (K-W, BKY).

Many glutamatergic synapses on cortical pyramidal cells do not respond to activation at resting membrane potential, yet they do have an NMDAR component that can be observed at Vhold=+50mV. After activation by LTP-evoking tetanic stimulation, these 'silent' synapses can convert to active, non-

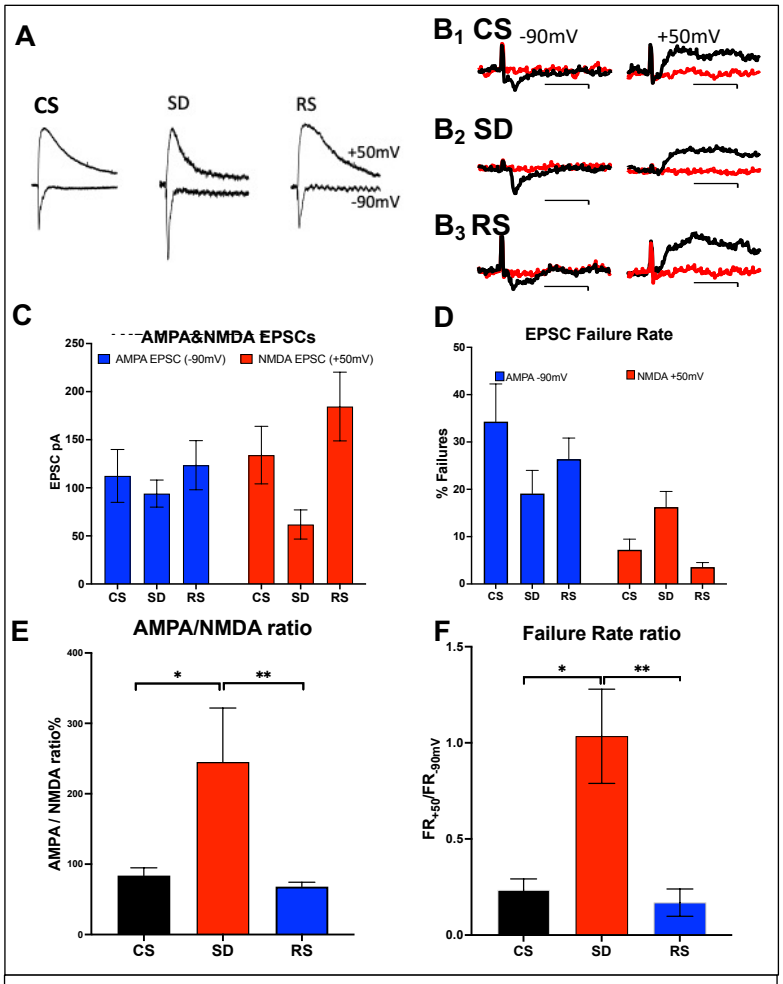

Figure 1. Sleep need-dependent responses of AMPA/NMDA ratio and silent synapses in motor cortex. **A)** Examples of AMPA currents at -90 mV holding potential and NMDA currents at +50 mV holding potential are shown for: control sleep (CS), 6 h of sleep deprivation (SD) and 4 h of sleep deprivation followed by 2 h of recovery sleep (RS). Traces (100msec duration) are scaled to the NMDA current for comparison (NMDA current measured @ 40msec after AMPA peak current). **B)** Examples of successes (black) and failures (red) at -90 mV (left, AMPA) and +50 mV (right, NMDA) after minimal stimulation of excitatory inputs to motor cortex pyramidal neurons are shown; Top row: CS sleep, middle row: SD and bottom row: RS (Cal. 10pAX20msec). Rate of failures (% of all stimuli delivered) for AMPA EPSCs (blue) and NMDA EPSCs (red) in the three conditions (+/- sem). **C), D)** Average (+/- sem) AMPAR and NMDAR EPSC responses (unmatched) and failure rates, respectively, for each sleep condition. **E), F)** Matched AMPA/NMDA response and AMPA/NMDA failure rate ratios, respectively, are shown for the three conditions (N=1-2 cells/slice/animal X 4animals for each condition).

silent synapses by virtue of LTP-induced AMPAR insertion into the post-synaptic active zone[8]. The ratio of AMPAR component failure rate (V_{hold}= -90mv; FR_{-90} for active synapses, As) matched with the same neuron's FR_{+50} (V_{hold}= +50mV; for As + silent synapses, Ss) has been used to estimate the change in the fraction of As (measured at V_{hold}= -90mv) to As+Ss (V_{hold}= +50mV) in response to LTP[8]. We employed a similar analysis to examine the effects of SD and sleep on functional synaptic AMPAR and NMDAR composition.

We observed a significant interaction between FR's and sleep conditions, assessed by a two-way ANOVA ($F(2, 18) = 5.433$ $p=0.0143$; Figure 1 $B_{1,2,3}$ D F). Multiple comparisons (K-Y BKY test) revealed no significant difference between FR_{-90} and FR_{+50} in SD indicating far fewer numbers of silent synapses (Ss) in this condition. However, both CS and RS restored the relatively decreased number of Ss compared to SD. FR_{-90} is significantly smaller than FR_{+50} for both CS and RS ($p<0.0001$ and <0.0007, respectively).

The condition specific ratio of FR_{+50mV} to FR_{-90mV} is a power function of the probability of failure for each of the stimulated synapses $(p_{failure})^{stimulated\text{-}synapse}$ and thus, inversely proportional (since $p_{failure}$ <1) to the number of silent synapses (Ss). Assuming a constant $p_{failure}$ for each synapse, the FR_{+50mV}/FR_{-90mV} = $(p_{failure})^{As+Ss}/(p_{failure})^{As}$ and $\ln(FR_{+50mV})/\ln(FR_{-90mV})$ =(As+Ss)/As=1+Ss/As. SD's FR_{+50mV}/FR_{-90mV}=~1 , indicating ~no silent synapses. The fraction Ss/As for CS=1.46 and for RS=1.50 . Thus, the near absence of silent synapses was reversed by either CS or RS

(K-W BKY test; p<0.01 comparing ratios SD/CS, p<0.001 for SD/RS; Figure 1 F). This suggests there are few if any silent synapses available for conversion by LTP to active synapses following SD and this availability is recovered by sleep.

The sleep-dependent electrophysiological findings raise several questions, including: 1) are other cell types besides the layer 2-3 pyramidal neurons from which we recorded, involved; 2) can changes in the transcriptome account, at least in part, for sleep-related synaptic changes in function, and if so, what are the specific functions of those genes and 3) what is the upstream sleep-dependent control of changes in gene expression?

To examine the molecular mechanisms responsible for an SD response, we characterized single nuclei transcriptomes of cells from motor cortex of mice from two cohorts, an ad lib or control sleep (CS) group and an SD group (sleep deprived from ZT= 0-6hr; see detailed methods).

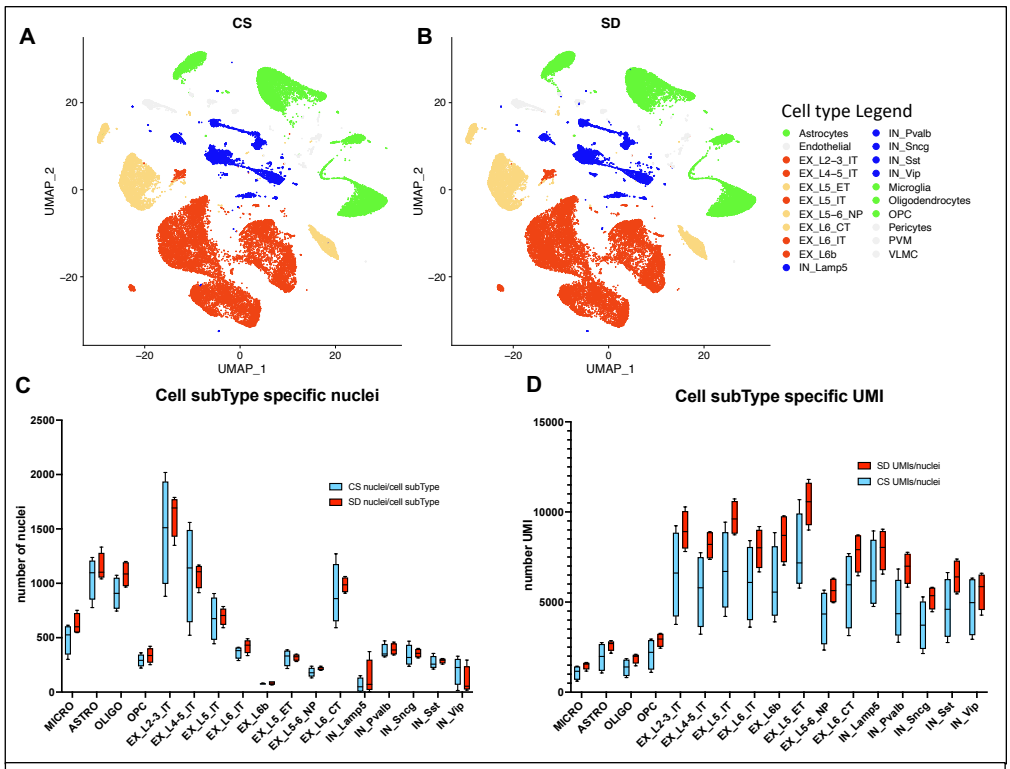

Figure 2. snRNAseq data shows cell type and sub-type based on gene expression patterns are unaffected by sleep need. **A)** UMAP projection of cell-type gene expression pattern following 6 hours ad lib sleep (CS) at ZT=6hour. **B)** As in "**A**" except after 6hours sleep deprivation (SD), ZT=6hour. **C)** The distribution of cell numbers across subtypes is unaffected by sleep need. **D)** The median number of UMIs/cell is significantly increased by sleep need across all cell subtypes (see table 2 and text for statistics).

Transcript libraries from each of the two cohorts (CS, n=4 and SD, n=4), were prepared from single nuclei isolated from mouse frontal cortex. Nuclei from each cohort were clustered and visualized using Uniform Manifold Approximation and Projection (UMAP) and annotated using multi-modal characteristics from the Brain Initiative Cell Census[9] (Figure 2 A,B). The sleep condition had no significant effect on the expression-based clustering nor on the distribution and numbers of nuclei per cell sub-type across sleep conditions (Figure 2 C). However, the SD condition was associated with a significantly increased number of transcripts/nucleus across sleep condition, matched for cell subtype (2way ANOVA, UMI/Nucleus(subType) x Condition(CSvsSD), F (16, 96) = 3.004, p=0.0004; Wilcoxon

matched-pairs, p<= 0.0001; Figure 2 D). To avoid any technical biases, the CS and SD biological samples were treated in an identical manner, with sacrifice alternating between CS and SD samples, carried out by the same person, brain harvesting and frontal cortex isolation all carried out by Dr. Richa Pandey, RIN values were indistinguishable and finally, library preparation and sequencing all completed as a single batch. Thus, the results may be indicative of a generalized increase in transcript number per cell sub-type.

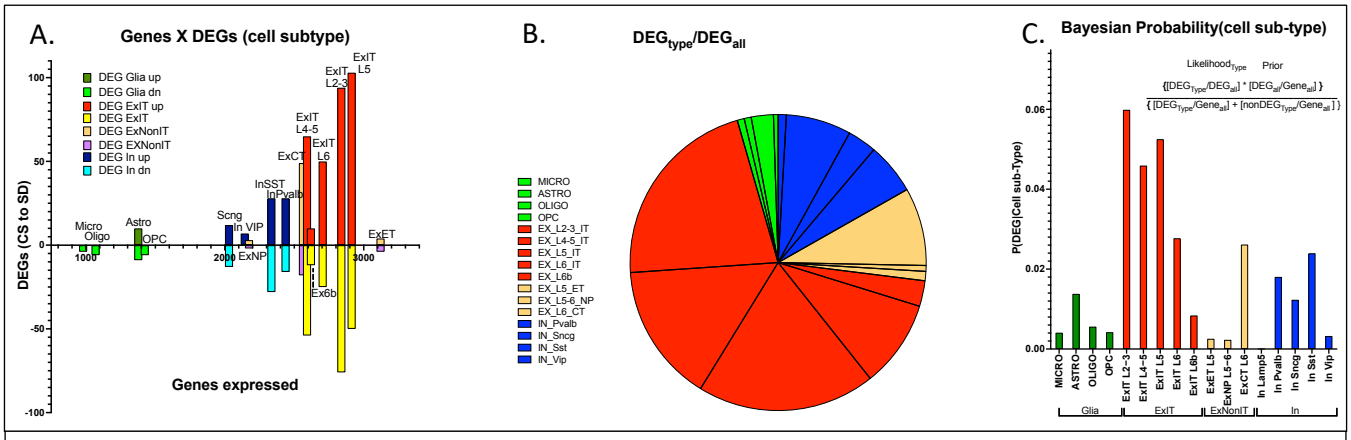

Figure 3. Cell type specific differential gene expression in response to 6 hours of SD. **A)** An XY bar plot of cell type specific DEGs (both up and down regulated) organized by cell type specific number of expressed genes (X axis) shows the greatest number of DEGs are found in excitatory pyramidal neurons that project within the telencephalon (ExIT). **B)** An analysis of the cell type specific DEG occurrence shows the greatest probability of significant sleep loss gene response is found in ExIT cells by more than 3-fold compared to all other cell types.

We next determined the differential gene expression (DGE) of transcripts between conditions of CS and SD (see methods; Figure 3 A). In response to 6 hours of SD from ZT= 0 to 6, both increased and decreased gene expression was observed in all cell subtypes (Table 2,3). Predictably, there is a trend for increased DEGs in cell types expressing a greater number of genes (Figure 3 A). The greatest proportion of sleep DEGs is ~69%, expressed by ExIT cell types, while the next largest proportion is ~17% for IN cell types (Figure 3 B). To determine whether the increased numbers of genes expressed in the ExIT subtypes accounts for this cell type's high proportion of DEGs, we examined each cell type's probability of DEG expression given the number of genes expressed in the cell type, its Bayesian probability of expression.

The Bayesian probability of sleep loss DEGs, for cell subtype, is more than three-fold greater for excitatory intratelencephalically projecting neurons (ExIT subtype, pyramidal cells[9]) compared to any other class of cells (Figure 3 C). These observations suggest, with respect to transcriptomic mediated changes in the frontal cortex, the ExIT class neurons comprise the major target of sleep function and extends earlier observations that frontal glutamatergic neurons are the primary targets of the SD transcriptomic response[7, 10].

We determined the functional relevance of cell-type specific DEGs with respect to both disease risk and biological properties. We found class-selective enrichment of both autism spectrum disorder genes (ASD; Figure 4 A) and synaptic shaping components[11] (Figure 4 A.).

Enrichment of sleep responsive DEGs by SSC and ASD genes, is strongest for ExIT (L 2-3, 4-5, 5) pyramidal neurons (Chi square with Yates correction p<0.006). In particular, a number of these sleep need ExIT-DEGs encode proteins that can directly affect AMPA/NMDA ratio and silent synapse numbers, including *Dcc*[12], *Dgkb*[13], *Gpc6*[14], *Grin3a*[15], *Kif17*[16, 17], *Kirrl3*[18] *and Ptprf*[19]. Some sleep modulated SSCs are also ASD risk factors in frontal cortical EXIT pyramidal neurons, including *Cdh13, Dcc, Glra2, Gpc6, Grik4, Itpr1, Kirrel3, Nr1d1, Pcdh15* and *Ush2a*. To a much lesser extent, Layer 6 corticothalamic pyramidal neurons

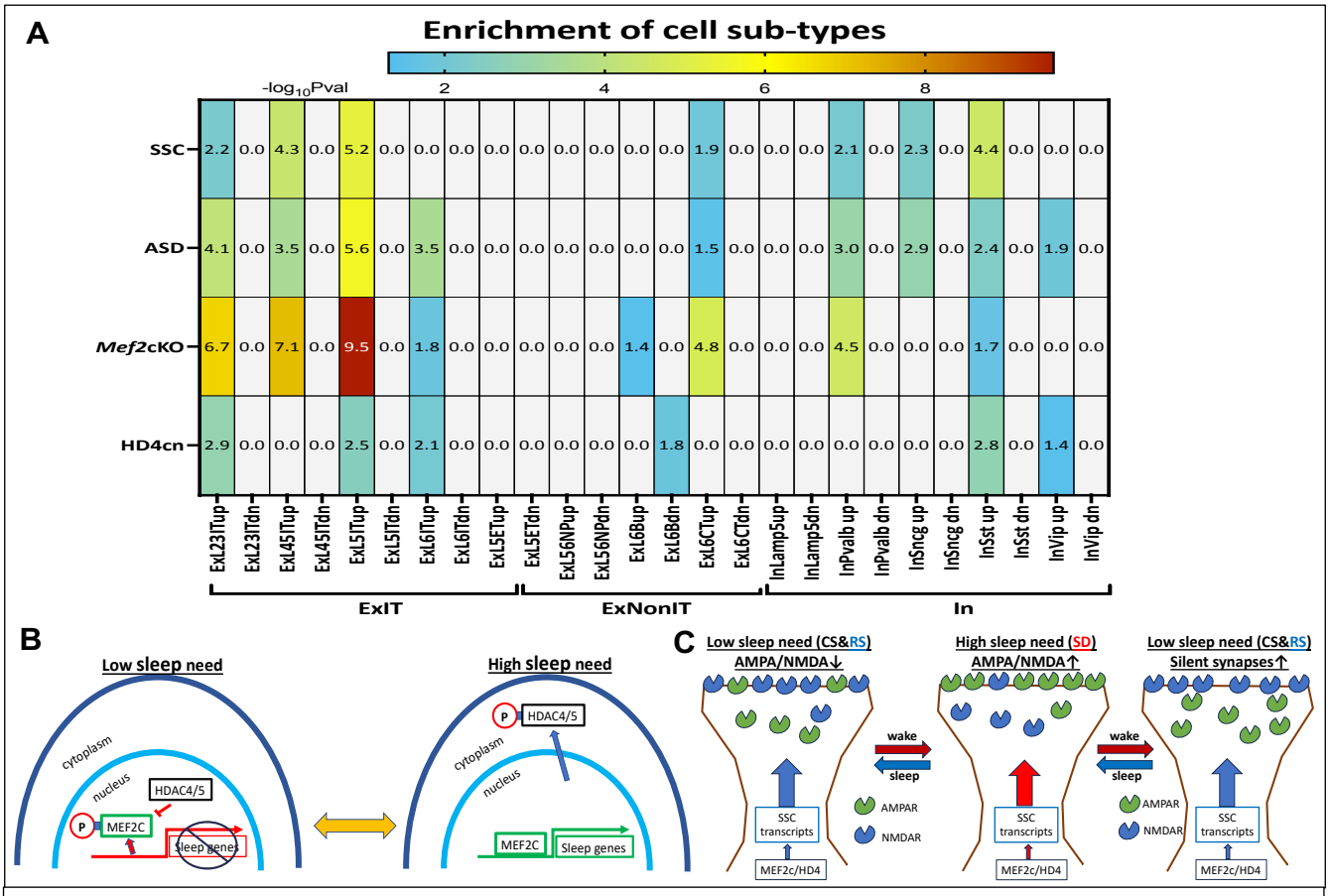

Figure 4. DEG enrichment of cell types in response to SD by autism risk genes, synaptic shaping component genes and DEGs from *MEF2c* loss of function or constitutive HD4 repression of MEF2c. **A)** Heat map for cell type DEG enrichment by ASD risk genes, Synaptic Shaping Component genes, *MEF2c*-cKO DEGs and HD4cn DEGs. **B)** Model for the control of sleep DEGs by HD4 repression of MEF2c and by pMEF2c during low sleep need and, during high sleep need, de-repression of MEF2c by sequestration of pHD4 to the cytoplasm and dephosphorylation of MEF2c, facilitating expression of sleep genes. **C)** Model of downstream control by MEF2c and HD4 to facilitate SSC gene expression as sleep need increases. The SSC gene expression after waking, can then decrease AMPA/NMDA ratio and increase silent synapses during sleep to bias glutamate synapses towards decreased strength but increased potential for LTP at the start of the active phase when sleep need is low.

and somatostatin, parvalbumin and *Sncg* classes of inhibitory neurons[20] also show this enrichment of their sleep DEGs (Figure 4 A). These observations are consistent with the ExIT pyramidal cell,

glutamatergic, synaptic phenotype as a major functional target for sleep proteins and implicates sleep (dis-)function's role in autism risk.

The transcription factor, MEF2c is necessary for sleep loss gene expression[7]. ExIT sleep loss genes are significantly ($p<0.0001$, Chi^2 with Yates correction) enriched with MEF2c target genes[7, 21] (Figure 4 A.) . Class II histone deacetylases 4/5 (HD4, HD5) are MEF2c binding partners and repressors[22], that can shuttle in and out of the nucleus and are trapped in the cytoplasm when phosphorylated by SIKinases (salt induced kinases[10, 23]), known to become active in conditions of high sleep need. As the mouse sleep phase progresses, HD4/5 is progressively de-phosphorylated in association with decreased sleep need and conversely as the mouse active phase progress, HD4/5 is progressively phosphorylated in association with increased sleep need (see Figure 4 in Zhou, et al.[23]). A virally-mediated expression of mutant form of HD4, that resists phosphorylation and is thus at constitutively high levels in the nucleus (*HD4cn*[23]), is expected to partially mimic a loss of function of *MEF2c* through constitutive repression of MEF2c. The sleep loss genes observed in frontal cortical ExIT neurons are enriched for both conditional *Mef2c*[7] loss of function DEGs ($p<0.0001$, Chi^2 with Yates correction) and for DEGs in response to expression of *HD4cn*[23] ($p<0.0001$, Chi^2 with Yates correction), as illustrated in a sleep-transcriptome expression model (Figure 4 B.). Further, these findings are indicative of the role of HD4 as a repressor of MEF2c facilitated sleep gene expression when sleep need is low and its de-repression of MEF2c through phosphorylation induced sequestration into the cytoplasm when sleep need is high[23]. The resulting high-sleep-need DEGs as noted above, can mediate the observed recovery of glutamate synapse phenotype from a high AMPA/NMDA ratio with sparse silent synapses to lowered AMPA/NMDA ratio and increased silent synapses (Figure 4 C).

Discussion

Prolonged waking is associated with increased glutamatergic synaptic strength[4, 7, 24] and increased number of functional AMPAR synapses[7]. Both effects are reversed by recovery sleep[7]. The evidence presented here suggests this wake/sleep homeostasis also reflects a waking induced increase in functional AMPA/NMDA ratio of glutamate synapses of the frontal cortex together with loss of silent glutamatergic synapses. The latter suggests a reduced availability of glutamate synapses for conversion from silent to active, reflecting saturation of LTP. Accordingly, it is reasonable to summarize the implications of sleep-related glutamate synaptic phenotype oscillation as: 1) prolonged waking induces a generalized synaptic strengthening coupled with a negative bias against potentiating plasticity and 2) a recovery by sleep (Figure 4 C).

Learning of motor tasks that can be robustly and quantitatively monitored, like bird song in juvenile zebra finches[25, 26], may reflect the sleep/wake oscillation of bias for LTP and synaptic strengthening. At the start of the active phase, facilitated motor learning improves song performance to a level that appears to saturate by the end of the day. After a night's sleep, performance is degraded but shows enhanced learning, facilitated by decreased AMPA/NMDA ratio and increased availability of synapses that can be readily potentiated. Since there are inevitable, day to day, unrelated variances in the environment that should not be learned, mitigation of over-fitting a learned task may require an oscillatory, stairstep-like, learning process. In rats, performance during learning of a novel motor task can display these similar characteristics, especially at the start of learning a novel task when exploration of a multi-dimensional

learning space is at a premium[27], consistent with an underlying sleep/wake oscillation of glutamate synaptic phenotype.

Our unbiased examination of the ontology of ExIT DEGs indicates a response to sleep loss to modify ExIT glutamate synapses can involve SSC DEGs. Our electrophysiological observations, now show more particularly, that the gene-expression modifications of ExIT neurons are coupled to SD-responses of, 1) increased AMPA/NMDA ratio; 2) decreased functional silent synapses and; 3) the previously described, increase in synaptic strength and functional number (Figures 1 and 4).

The ontology of the ExIT SD-response transcriptome is also notable for enrichment by autism-related risk genes, many of which overlap with our curated category of SSCs. A similar overlap has been noted for social affiliative behaviors, synaptic adhesion molecules, other synaptic shaping molecules with autism/autism spectrum disorder (ASD) risk genes in the mammalian CNS[28]. The association of sleep disruption with autism is generally appreciated[29] but the focus was on loss of time spent asleep or disrupted sleep, rather than loss of sleep function. The overlapped SSC and ASD DEGs provide a molecular association between sleep's functional role in motor cortex and ASD risk that captures ASD's association with motor deficits observed in patients[30] and in mouse autism models[31].

The molecular mechanisms responsible for sleep/wake DEGs observed in ExIT neurons include two critical transcription factors, MEF2c[7] and HD4/5[10, 23]. All neuronal and non-neuronal frontal cortical transcriptomic changes are abolished by loss of function of *Mef2c*[7]. The abolishment of the sleep transcriptome remained even after restriction of the *Mef2c* knockout to *CamKII*-expressing glutamatergic neurons of the forebrain. Importantly, MEF2c was necessary for both the SD-transcriptomic response and for SD-induced increase of glutamatergic synaptic strength and functional synaptic number as well as for ensuing sleep-mediated recovery[7] . Thus, MEF2c has an essential role in facilitating the expression of sleep genes needed for recovery from loss of sleep.

The activity of either of these factors to alter the sleep transcriptome, is controlled by their phosphorylation state. When sleep need is high, MEF2c is de-phosphorylated[7] (from pMEF2c to MEF2c) and Salt Induced Kinases (SIKs) phosphorylate HD4 and HD5 (pHD4/5), trapping them in the cytoplasm[10, 23]. Both the phosphorylation of HD4/5s[32] and de-phosphorylation of MEF2c[33], de-represses MEF2c transcriptional activity. The de-repression of MEF2c and its dephosphorylation are essential for SD-induced differential expression[7]. The target genes of MEF2c activation can be inferred from the cortical, differential transcriptome induced by MEF2c loss of function[21]. These same genes overlap with the differentially expressed genes observed in response to overexpression of constitutively nuclear HD4 (HD4cn). This is predictable as HD4cn will constitutively bind and repress MEF2c in the nucleus, thus mimicking a MEF2c loss of function. Furthermore, in association with low sleep need, nuclear, and thus transcriptionally active (as a repressor), HD4, is more abundant in a de-phosphorylated state, relative to transcriptionally inactive, phosphorylated cytoplasmic pHD4[10, 23]. NMDAR activation negatively controls HD4 transcriptional activity and nuclear localization[34]. Accordingly, as NMDAR activity accumulates during the active period, an expected accumulation of pHD4 in the cytoplasm occurs to derepress MEF2c activity. Thus, HD4 may act to repress MEF2c transcriptional facilitation of sleep genes, during low sleep need and derepress MEF2c as sleep need builds during the active period. We observed DEGs from both

MEF2c loss of function and HD4cn also sleep DEGs consistent with their interaction driven by sleep need (Figure 4 C.).

Both the role of MEF2c to mediate sleep gene expression and nuclear HD4 to repress MEF2c activity, lead to an apparent paradox. When HD4 repression of MEF2c is chronically reduced or lost, sleep need, as indicated by slow wave activity during slow wave sleep (SWS-SWA), is increased[10]. If MEF2c promotes sleep gene expression, then sleep need should be reduced not increased by its de-repression. Conversely, when nuclear HD4 is overexpressed, thus chronically repressing MEF2c, sleep need, as indicated by SWS-SWA, is unexpectedly, reduced[23]. But, what is actually being indicated by SWS-SWA?

SWS-SWA has long been employed as a marker for sleep need or intensity, primarily because of its strong correlation with previous time spent awake[35, 36]. Despite this marker's long history, the mechanisms responsible for its correlation to sleep need are not well understood. A likely candidate is adenosine (Ado) since, it is increased by sleep-need and is necessary for SWS-SWA rebound in response to SD[37]. Ado is increased by glutamate synaptic activity acting on NMDARs in arousal centers. Ado activation of Ado A1 receptors (ADORA1) inhibits AMPAR synaptic activity[38, 39]. *Adk*, which encodes adenosine kinase in glial cells is the high affinity metabolizing enzyme of Ado. Glial knockout of *Adk* increases extracellular Ado and SWA in both wake and sleep[40]. Rebound SWS-SWA in response to experimental SD increases Ado[37] and the rebound is blocked by a *CamKII:Cre* driven conditional knockout of *Adora1*[40]. Thus Ado, through its activation of ADORA1, inhibits glutamate synaptic activity, including in arousal centers, to promote SWS-SWA[39].

Sleep, itself, induces a down-regulation of glutamate synaptic strength, synaptic numbers, and AMPA/NMDA ratio. Chronic facilitation of MEF2c-dependent sleep genes due to de-repression of MEF2c by HD4/5's loss of function should induce a chronic down-regulation of glutamatergic synaptic drive[10, 23]. This down-regulation can mimic Ado's effect as observed with chronic loss of function of *Adk* that chronically increases extracellular Ado and SWS-SWA[40].

Conversely, chronic disruptions of sleep mediated transcription by *MEF2c* loss of function, blocks sleep-induced down-regulation of frontal cortical glutamatergic synapses[7]. This can mimic *Adora1* loss of function that attenuates SWS-SWA[7, 40]. Similarly, repression of MEF2c by de-phosphorylated HD4/5 (or by expression of phospho-dead HD4cn) reduces SWS-SWA[23]. However, while a loss of function of *Mef2c* in glutamate neurons prevents sleep gene expression[7], HD4cn's effect on sleep gene expression in response to SD remains to be examined.

In summary, at the end of a long episode of waking, when sleep need is high, glutamate synapses of ExIT cells in the frontal cortex are electro-physiologically strengthened, increased in functional number, and show increased AMPA/NMDA ratio, together with decreased availability of silent synapses. The silent synapse conversion by LTP to active synapses is thus limited, creating a bias for increased strength at the expense of potentiating plasticity. In the ExIT neuronal nuclei, the transcription factor, MEF2c is de-repressed by de-phosphorylation and sequestration of its co-repressors, the classII HDACs, pHD4/5, to the cytoplasm. This facilitates transcription of sleep genes, including those encoding SSCs controlling glutamatergic synaptic phenotype and ASD risk genes. Recovery sleep recovers the functional phenotype. These observations suggest a daily oscillation from lowered glutamatergic synaptic strength and increased bias for potentiating plasticity at the start of the active phase when sleep need is low, to

increased synaptic strength and saturated plasticity at the end of the active phase, when sleep need is high. In conclusion, we have provided electrophysiological evidence for a wake/sleep oscillation of glutamate synapse phenotype that can mediate a glutamatergic strength/plasticity oscillating bias. We also show that this wake/sleep oscillation is likely to occur in glutamate synapses of ExIT pyramidal neurons and be mediated by a select set of synaptic shaping component genes, a significant number of which are also autism risk genes, whose expression is controlled by MEF2C and HD4 transcription factors. Finally, this study implicates a framework within which optimal cortical-dependent motor training can occur in a recursive incremental manner, facilitated by wake/sleep glutamate synapse phenotypical oscillation.

Figure Legends

Figure 1. Sleep need-dependent responses of AMPA/NMDA ratio and silent synapses in motor cortex. **A)** Examples of AMPA currents at -90 mV holding potential and NMDA currents at +50 mV holding potential are shown for: control sleep (CS), 6 h of sleep deprivation (SD) and 4 h of sleep deprivation followed by 2 h of recovery sleep (RS). Traces (100msec duration) are scaled to the NMDA current for comparison (NMDA current measured @ 40msec after AMPA peak current). **B)** Examples of successes (black) and failures (red) at -90 mV (left, AMPA) and +50 mV (right, NMDA) after minimal stimulation of excitatory inputs to motor cortex pyramidal neurons are shown; Top row: CS sleep, middle row: SD and bottom row: RS (Cal. 10pAX20msec). Rate of failures (% of all stimuli delivered) for AMPA EPSCs (blue) and NMDA EPSCs (red) in the three conditions (+/- sem). **C), D)** Average (+/- sem) AMPAR and NMDAR EPSC responses (unmatched) and failure rates, respectively, for each sleep condition. **E), F)** Matched AMPA/NMDA response and AMPA/NMDA failure rate ratios, respectively, are shown for the three conditions (N=1-2 cells/slice/animal X 4animals for each condition).

Figure 2. snRNAseq data shows cell type and sub-type based on gene expression patterns are unaffected by sleep need. **A)** UMAP projection of cell-type gene expression pattern following 6 hours ad lib sleep (CS) at ZT=6hour. **B)** As in "**A**" except after 6hours sleep deprivation (SD), ZT=6hour. **C)** The distribution of cell numbers across subtypes is unaffected by sleep need. **D)** The median number of UMIs/cell is significantly increased by sleep need across all cell subtypes (see table 2 and text for statistics).

Figure 3. Cell type specific differential gene expression in response to 6 hours of SD. **A)** An XY bar plot of cell type specific DEGs (both up and down regulated) organized by cell type specific number of expressed genes (X axis) shows the greatest number of DEGs are found in excitatory pyramidal neurons that project within the telencephalon (ExIT). **B)** An analysis of the cell type specific DEG occurrence shows the greatest probability of significant sleep loss gene response is found in ExIT cells by more than 3-fold compared to all other cell types.

Figure 4. DEG enrichment of cell types in response to SD by autism risk genes, synaptic shaping component genes and DEGs from *MEF2c* loss of function or constitutive HD4 repression of MEF2c. **A)** Heat map for cell type DEG enrichment by ASD risk genes, Synaptic Shaping Component genes, *MEF2c*-cKO DEGs and HD4cn DEGs. **B)** Model for the control of sleep DEGs by HD4 repression of MEF2c and by pMEF2c during low sleep need and, during high sleep need, de-repression of MEF2c by sequestration of pHD4 to the cytoplasm and dephosphorylation of MEF2c, facilitating expression of sleep genes. **C)** Model of downstream control by MEF2c and HD4 to facilitate SSC gene expression as sleep need increases. The SSC gene expression after waking, can then decrease AMPA/NMDA ratio and increase silent synapses during sleep to bias glutamate synapses towards decreased strength but increased potential for LTP at the start of the active phase when sleep need is low.

Methods
Electrophysiology:

All electrophysiological animal experiments were approved by the Animal Experimental Committee at the University of Tsukuba. Animals were housed on a 12:12-h light/dark cycle (with the light automatically turned on at 9:00) at a stable temperature (24.5 ± 0.5 °C), with free access to food and water. C57/Bl6 male mice aged 8 to 12 weeks were used.

Slice preparation and recording

Mice were fully anesthetized at ZT 6 with isoflurane, and their brains were promptly removed (<1 min) and placed in ice-cold artificial cerebrospinal fluid (ACSF), composed of 124 mM NaCl, 26 mM NaHCO3, 3 mM KCl, 2 mM CaCl, 1 mM MgSO4, 1.25 mM KH2PO4, 10 mM glucose, 300 to 310 mOsm, equilibrated with 95% O2 and 5% CO2.

Brains were mounted on the stage of a vibrating microtome (Leica VT1200 S) with cyanoacrylate glue. Coronal sections (300 µm thick) were obtained and allowed to recover in ACSF at room temperature for at least 1 h. Slices were submerged in a perfusion chamber placed under an upright microscope (BX51WI; Olympus) fitted with a custom LED IR illumination and Nomarski interference contrast. Slices were superfused with ACSF, at a rate of 2 mL/min with Picrotoxin (100 micromolar) added to block $GABA_A$ receptor-mediated responses. Neurons in layers 2/3 of primary motor cortex with a pyramidal cell morphology were patched under visual control. The intracellular solution contained (in mM) 130 Cs gluconate, 1 mM EGTA, 10 mM Hepes, 4 mM MgATP, 0.3 mM NaGTP, and 5 mM NaCl. The pH was adjusted to 7.33 with CsOH and osmolarity to 285 to 300 mOsm. Borosilicate patch pipettes were pulled to an open-tip resistance of 2 to 4 MΩ. Signals were amplified and filtered at 10 kHz (Axopatch 700A; Molecular Devices) and then digitized at 20 kHz using customized routines in commercial software (IGOR Pro; WaveMetrics). Evoked synaptic responses were produced through extracellular stimulation (0.1 ms) every 10 s with monopolar glass pipette electrodes filled with ACSF and placed in the vicinity (200-400 micrometers) lateral to the recorded neuron in layer 2/3.

AMPA/NMDA EPSCs: AMPA responses were recorded at a holding potential of -90 mV and mixed AMPA-NMDA responses at a holding potential of +50 mV. The AMPA/NMDA ratio was determined according to an established protocol[41]; briefly, at least 10 traces were averaged at -90 mV and +50 mV, the AMPA response was calculated as the peak inward current at -90 mV and the NMDA current was calculated at +50 mV in a 5 ms window 40 ms after the AMPA peak.

Failure rates for AMPA and AMPA+NMDA EPSCs: Minimal stimulation was achieved by lowering the stimulation strength until clear successes and failures could be observed at -90 mV holding potential and stimulation strength was then kept constant for 5-10 min to allow the system to stabilize before failure ratios were determined. Relative numbers of silent and total (silent + active) synapse in an L2-3 pyramidal neuron evoked in a slice by minimal presynaptic stimulation are correlated with failure rates (FR= failures/number of stimuli). $FR_{-90} = (p_{failure})^{As}$, and $FR_{+50} = (p_{failure})^{As+Ss}$, where As=number active synapses (at -90mV) and Ss= number of silent synapses (those only active at +50mV). Since $p_{failure}$ for each synapse is the same for -90mV and +50mV (assuming the same probability of failure at both potentials with each stimulus) then $(FR_{+50}/FR_{-90}) = (p_{failure})^{Ss}$. Note as Ss-->0, (FR_{+50}/FR_{-90})--> 1, the maximal ratio possible if

$p_{failure}$ is constant. Our uncorrected data show (FR_{+50}/FR_{-90})=~1.3 in SD, which suggests that FR_{+50} is overestimated by at least a factor of 1.3 (likely as a result of decreased input resistance at Vh=+50mV). Accordingly, we adjusted FR_{+50} by this factor for all conditions.

Sleep deprivation

All mice were accommodated for 1-2 weeks to a cage and treadmill, consisting of a bottomless plexiglass enclosure suspended over the treadmill with ad lib access to food and water. For sleep deprivation (SD) the slow-moving treadmill (0.1KM/hour) was engaged from ZT 0-6 hours and for recovery sleep (RS) from ZT 0-4. There was no treadmill engagement for RS from ZT 4-6 hours and for control sleep (CS), no treadmill engagement for the entire ZT 0-6 hours period. All animals were sacrificed at ZT=6 hours and tissue rapidly prepared for either electrophysiological (*exVivo* brain slices) or transcriptomic analysis as described below.

Single nucleus Transcriptome analysis:

snRNA-seq library preparation

Nuclei for snRNA-seq were isolated from mice, 8-10 weeks old. Briefly, the tissue was homogenized using a glass Dounce homogenizer in 2 ml of ice-cold lysis buffer (10 mM Tris-HCl, 10 mM NaCl, 3 mM $MgCl_2$ and 0.1% Nonidet P40 Substitute) and was incubated on ice for 5 min. Nuclei were centrifuged at 500*g* for 5 min at 4 °C, washed with 4 ml ice-cold lysis buffer and incubated on ice for 5 min. Nuclei were centrifuged at 500*g* for 5 min at 4 °C. After centrifugation, the nuclei were resuspended in 500 µl of nucleus suspension buffer (NSB) containing 1× PBS, 1% BSA (no. AM2618, Thermo Fisher Scientific) and 0.2 U μl^{-1} RNAse inhibitor (no. AM2694, Thermo Fisher Scientific). The nucleus suspension was filtered through a 70-µm Flowmi cell strainer (no. H13680-0070, Bel-Art). Debris was removed with density gradient centrifugation using Nuclei PURE 2 M sucrose cushion solution and Nuclei PURE sucrose cushion buffer from the Nuclei PURE prep isolation kit (no. NUC201-1KT, Sigma Aldrich). Nuclei PURE 2 M sucrose cushion solution and Nuclei PURE sucrose cushion buffer were first mixed in a 9:1 ratio. A 500 µl volume of the resulting sucrose solution was added to a 2-ml Eppendorf tube. A 900 µl volume of the sucrose buffer was added to 500 µl of isolated nuclei in NSB. A 1,400 µl volume of nucleus suspension was layered to the top of the sucrose buffer. This gradient was centrifuged at 13,000*g* for 45 min at 4 °C. The pellet of nuclei was resuspended, washed once in NSB and filtered through a 70-µm Flowmi cell strainer (no. H13680-0070, Bel-Art). The concentration of nuclei was determined using 0.4% trypan blue (no. 15250061, Thermo Fisher Scientific), and was adjusted to a final concentration of 1,000 nuclei per microlitre with NSB.

Droplet-based snRNA-seq libraries were prepared using Chromium Single Cell 3' v3.1 (1000121, 10x Genomics) according to the manufacturer's protocol[42]. Libraries were sequenced using an Illumina NovaSeq 6000.

snRNA-seq preprocessing and annotationRaw sequencing data was obtained as BCL files from the McDermott sequencing core at UT Southewestern. BCL files were demultiplexed using *cellranger mkfastq*

(10X Genomics CellRanger suite v3.1.0). Resulting FASTQ files were then accessed for quality using FASTQC (v0.11.5). A reference mouse genome-annotation index was built for mouse genome (GRCm38p6) and Gencode annotation (vM17) using *cellranger mkref* (10X Genomics CellRanger suite v3.1.0). Quality passed FASTQ files were further aligned to reference mouse genome-annotation index and raw count matrices were generated using *cellranger count* (10X Genomics CellRanger suite v3.1.0).

To remove ambient RNA contamination, we used CellBender's *remove-background* (https://github.com/broadinstitute/CellBender) on the raw count matrix per sample. We note that without ambient RNA removal, glial cells were shown to be conspicuously contaminated with neuronal ambient RNAs[43]. Also, potential doublets were discarded using DoubletFinder (https://github.com/chris-mcginnis-ucsf/DoubletFinder) tool.

Ambient RNA and doublets cleaned data were used for downstream analysis. For each sample, nuclei with less than 20,000 UMIs and percentage of reads mapping to mitochondrial genes of less then 0.5 were retained. Individual samples per sleep condition were first integrated using Seurat's (v3) integration approach (*IntegrateData*) and integrated datasets were further clustered (*ScaleData*, *RunPCA*, *FindClusters*) as described in Seurat's (v3) integration vignette (https://satijalab.org/seurat/archive/v3.0/integration). Clustered data was then visualized (*RunUMAP*) using Uniform manifold approximation and projection embeddings (UMAP). Cluster-specific gene markers were identified (*FindMarkers*) and significant marker genes were enriched using Fisher exact test for cell-type markers defined in Brain Initiative Cell Census to annotate the cell-types. Cell-types were also confirmed by expression of canonical marker genes.

Differential gene expression tests were performed using edgeR-based pseudobulk approach across sleep conditions per cell-type. Significant differentially expressed genes (DEGs) were identified using absolute log2 fold change >= 0.1375 (10%) and a false discovery rate (FDR) <= 0.05. Further significant DEGs were enriched across defined gene classes (such as SSC genes, ASD genes, Mef2c-cKO genes and HD4cn genes) using R package *SuperExactTest* to functionally annotate the genes.

Bibliography

1. Morris RG, Moser EI, Riedel G, Martin SJ, Sandin J, Day M, O'Carroll C. Elements of a neurobiological theory of the hippocampus: the role of activity-dependent synaptic plasticity in memory. PhilosTransRSocLond B BiolSci. 2003;358(1432):773-86.
2. Moser EI, Krobert KA, Moser MB, Morris RG. Impaired spatial learning after saturation of long-term potentiation. Science. 1998;281(5385):2038-42. Epub 1998/09/25. doi: 10.1126/science.281.5385.2038. PubMed PMID: 9748165.
3. Stickgold R. Sleep-dependent memory consolidation. Nature. 2005;437(7063):1272-8. doi: 10.1038/nature04286. PubMed PMID: 16251952.
4. Liu ZW, Faraguna U, Cirelli C, Tononi G, Gao XB. Direct evidence for wake-related increases and sleep-related decreases in synaptic strength in rodent cortex. The Journal of neuroscience : the official journal of the Society for Neuroscience. 2010;30(25):8671-5. doi: 10.1523/JNEUROSCI.1409-10.2010. PubMed PMID: 20573912; PMCID: 2903226.
5. Torrado Pacheco A, Bottorff J, Gao Y, Turrigiano GG. Sleep Promotes Downward Firing Rate Homeostasis. Neuron. 2021;109(3):530-44 e6. Epub 20201123. doi: 10.1016/j.neuron.2020.11.001. PubMed PMID: 33232655; PMCID: PMC7864886.
6. Tononi G, Cirelli C. Sleep and the price of plasticity: from synaptic and cellular homeostasis to memory consolidation and integration. Neuron. 2014;81(1):12-34. doi: 10.1016/j.neuron.2013.12.025. PubMed PMID: 24411729; PMCID: 3921176.
7. Bjorness TE, Kulkarni A, Rybalchenko V, Suzuki A, Bridges C, Harrington AJ, Cowan CW, Takahashi JS, Konopka G, Greene RW. An essential role for MEF2C in the cortical response to loss of sleep in mice. Elife. 2020;9. doi: 10.7554/eLife.58331. PubMed PMID: 32851972; PMCID: PMC7490011.
8. Liao D, Hessler NA, Malinow R. Activation of postsynaptically silent synapses during pairing-induced LTP in CA1 region of hippocampal slice. Nature. 1995;375(6530):400-4. PubMed PMID: 6770.
9. Network BICC. A multimodal cell census and atlas of the mammalian primary motor cortex. Nature. 2021;598(7879):86-102. Epub 2021/10/08. doi: 10.1038/s41586-021-03950-0. PubMed PMID: 34616075; PMCID: PMC8494634.
10. Kim SJ, Hotta-Hirashima N, Asano F, Kitazono T, Iwasaki K, Nakata S, Komiya H, Asama N, Matsuoka T, Fujiyama T, Ikkyu A, Kakizaki M, Kanno S, Choi J, Kumar D, Tsukamoto T, Elhosainy A, Mizuno S, Miyazaki S, Tsuneoka Y, Sugiyama F, Takahashi S, Hayashi Y, Muratani M, Liu Q, Miyoshi C, Yanagisawa M, Funato H. Kinase signalling in excitatory neurons regulates sleep quantity and depth. Nature. 2022;612(7940):512-8. Epub 20221207. doi: 10.1038/s41586-022-05450-1. PubMed PMID: 36477539.
11. Koopmans F, van Nierop P, Andres-Alonso M, Byrnes A, Cijsouw T, Coba MP, Cornelisse LN, Farrell RJ, Goldschmidt HL, Howrigan DP, Hussain NK, Imig C, de Jong APH, Jung H, Kohansalnodehi M, Kramarz B, Lipstein N, Lovering RC, MacGillavry H, Mariano V, Mi H, Ninov M, Osumi-Sutherland D, Pielot R, Smalla KH, Tang H, Tashman K, Toonen RFG, Verpelli C, Reig-Viader R, Watanabe K, van Weering J, Achsel T, Ashrafi G, Asi N, Brown TC, De Camilli P, Feuermann M, Foulger RE, Gaudet P, Joglekar A, Kanellopoulos A, Malenka R, Nicoll RA, Pulido C, de Juan-Sanz J, Sheng M, Sudhof TC, Tilgner HU, Bagni C, Bayes A, Biederer T, Brose N, Chua JJE, Dieterich DC, Gundelfinger ED, Hoogenraad C, Huganir RL, Jahn R, Kaeser PS, Kim E, Kreutz MR, McPherson PS, Neale BM, O'Connor V, Posthuma D, Ryan TA, Sala C, Feng G, Hyman SE, Thomas PD, Smit AB, Verhage M. SynGO: An Evidence-Based, Expert-Curated Knowledge Base for the Synapse. Neuron. 2019;103(2):217-34 e4. Epub 20190603. doi: 10.1016/j.neuron.2019.05.002. PubMed PMID: 31171447; PMCID: PMC6764089.

12. Horn KE, Glasgow SD, Gobert D, Bull SJ, Luk T, Girgis J, Tremblay ME, McEachern D, Bouchard JF, Haber M, Hamel E, Krimpenfort P, Murai KK, Berns A, Doucet G, Chapman CA, Ruthazer ES, Kennedy TE. DCC expression by neurons regulates synaptic plasticity in the adult brain. Cell reports. 2013;3(1):173-85. Epub 20130103. doi: 10.1016/j.celrep.2012.12.005. PubMed PMID: 23291093.
13. Kakefuda K, Ishisaka M, Tsuruma K, Shimazawa M, Hara H. Memantine, an NMDA receptor antagonist, improves working memory deficits in DGKbeta knockout mice. Neurosci Lett. 2016;630:228-32. Epub 20160802. doi: 10.1016/j.neulet.2016.07.061. PubMed PMID: 27495014.
14. Sato K, Takahashi K, Shigemoto-Mogami Y, Chujo K, Sekino Y. Glypican 6 Enhances N-Methyl-D-Aspartate Receptor Function in Human-Induced Pluripotent Stem Cell-Derived Neurons. Front Cell Neurosci. 2016;10:259. Epub 20161115. doi: 10.3389/fncel.2016.00259. PubMed PMID: 27895553; PMCID: PMC5108764.
15. Perez-Otano I, Larsen RS, Wesseling JF. Emerging roles of GluN3-containing NMDA receptors in the CNS. Nat Rev Neurosci. 2016;17(10):623-35. Epub 20160825. doi: 10.1038/nrn.2016.92. PubMed PMID: 27558536.
16. Iwata S, Morikawa M, Takei Y, Hirokawa N. An activity-dependent local transport regulation via degradation and synthesis of KIF17 underlying cognitive flexibility. Sci Adv. 2020;6(51). Epub 20201216. doi: 10.1126/sciadv.abc8355. PubMed PMID: 33328231; PMCID: PMC7744090.
17. Setou M, Nakagawa T, Seog DH, Hirokawa N. Kinesin superfamily motor protein KIF17 and mLin-10 in NMDA receptor-containing vesicle transport. Science. 2000;288(5472):1796-802. doi: 10.1126/science.288.5472.1796. PubMed PMID: 10846156.
18. Martin EA, Muralidhar S, Wang Z, Cervantes DC, Basu R, Taylor MR, Hunter J, Cutforth T, Wilke SA, Ghosh A, Williams ME. The intellectual disability gene Kirrel3 regulates target-specific mossy fiber synapse development in the hippocampus. Elife. 2015;4:e09395. Epub 20151117. doi: 10.7554/eLife.09395. PubMed PMID: 26575286; PMCID: PMC4642954.
19. Sclip A, Sudhof TC. LAR receptor phospho-tyrosine phosphatases regulate NMDA-receptor responses. Elife. 2020;9. Epub 20200127. doi: 10.7554/eLife.53406. PubMed PMID: 31985401; PMCID: PMC6984820.
20. Scala F, Kobak D, Bernabucci M, Bernaerts Y, Cadwell CR, Castro JR, Hartmanis L, Jiang X, Laturnus S, Miranda E, Mulherkar S, Tan ZH, Yao Z, Zeng H, Sandberg R, Berens P, Tolias AS. Phenotypic variation of transcriptomic cell types in mouse motor cortex. Nature. 2021;598(7879):144-50. Epub 2020/11/14. doi: 10.1038/s41586-020-2907-3. PubMed PMID: 33184512; PMCID: PMC8113357.
21. Harrington AJ, Raissi A, Rajkovich K, Berto S, Kumar J, Molinaro G, Raduazzo J, Guo Y, Loerwald K, Konopka G, Huber KM, Cowan CW. MEF2C regulates cortical inhibitory and excitatory synapses and behaviors relevant to neurodevelopmental disorders. Elife. 2016;5. doi: 10.7554/eLife.20059. PubMed PMID: 27779093.
22. McKinsey TA, Zhang CL, Lu J, Olson EN. Signal-dependent nuclear export of a histone deacetylase regulates muscle differentiation. Nature. 2000;408(6808):106-11. doi: 10.1038/35040593. PubMed PMID: 11081517; PMCID: PMC4459600.
23. Zhou R, Wang G, Li Q, Meng F, Liu C, Gan R, Ju D, Liao M, Xu J, Sang D, Gao X, Zhou S, Wu K, Sun Q, Guo Y, Wu C, Chen Z, Chen L, Shi B, Wang H, Wang X, Li H, Cai T, Li B, Wang F, Funato H, Yanagisawa M, Zhang EE, Liu Q. A signalling pathway for transcriptional regulation of sleep amount in mice. Nature. 2022;612(7940):519-27. Epub 20221207. doi: 10.1038/s41586-022-05510-6. PubMed PMID: 36477534.

24. Vyazovskiy VV, Cirelli C, Pfister-Genskow M, Faraguna U, Tononi G. Molecular and electrophysiological evidence for net synaptic potentiation in wake and depression in sleep. NatNeurosci. 2008;11(2):200-8.
25. Deregnaucourt S, Mitra PP, Feher O, Pytte C, Tchernichovski O. How sleep affects the developmental learning of bird song. Nature. 2005;433(7027):710-6. doi: 10.1038/nature03275. PubMed PMID: 15716944.
26. Kollmorgen S, Hahnloser RHR, Mante V. Nearest neighbours reveal fast and slow components of motor learning. Nature. 2020;577(7791):526-30. Epub 20200108. doi: 10.1038/s41586-019-1892-x. PubMed PMID: 31915383; PMCID: PMC7610670.
27. Kim J, Joshi A, Frank L, Ganguly K. Cortical-hippocampal coupling during manifold exploration in motor cortex. Nature. 2023;613(7942):103-10. Epub 20221214. doi: 10.1038/s41586-022-05533-z. PubMed PMID: 36517602; PMCID: PMC9812770.
28. Taylor SC, Ferri SL, Grewal M, Smernoff Z, Bucan M, Weiner JA, Abel T, Brodkin ES. The Role of Synaptic Cell Adhesion Molecules and Associated Scaffolding Proteins in Social Affiliative Behaviors. Biol Psychiatry. 2020;88(6):442-51. Epub 20200222. doi: 10.1016/j.biopsych.2020.02.012. PubMed PMID: 32305215; PMCID: PMC7442706.
29. Mazurek MO, Dovgan K, Neumeyer AM, Malow BA. Course and Predictors of Sleep and Co-occurring Problems in Children with Autism Spectrum Disorder. J Autism Dev Disord. 2019;49(5):2101-15. doi: 10.1007/s10803-019-03894-5. PubMed PMID: 30684086.
30. Chukoskie L, Townsend J, Westerfield M. Motor skill in autism spectrum disorders: a subcortical view. International review of neurobiology. 2013;113:207-49. doi: 10.1016/B978-0-12-418700-9.00007-1. PubMed PMID: 24290387.
31. Cording KR, Bateup HS. Altered motor learning and coordination in mouse models of autism spectrum disorder. Front Cell Neurosci. 2023;17:1270489. Epub 20231108. doi: 10.3389/fncel.2023.1270489. PubMed PMID: 38026686; PMCID: PMC10663323.
32. Miska EA, Karlsson C, Langley E, Nielsen SJ, Pines J, Kouzarides T. HDAC4 deacetylase associates with and represses the MEF2 transcription factor. The EMBO journal. 1999;18(18):5099-107. doi: 10.1093/emboj/18.18.5099. PubMed PMID: 10487761; PMCID: PMC1171580.
33. Zhu B, Gulick T. Phosphorylation and alternative pre-mRNA splicing converge to regulate myocyte enhancer factor 2C activity. Mol Cell Biol. 2004;24(18):8264-75. doi: 10.1128/MCB.24.18.8264-8275.2004. PubMed PMID: 15340086; PMCID: PMC515034.
34. Sando R, 3rd, Gounko N, Pieraut S, Liao L, Yates J, 3rd, Maximov A. HDAC4 governs a transcriptional program essential for synaptic plasticity and memory. Cell. 2012;151(4):821-34. doi: 10.1016/j.cell.2012.09.037. PubMed PMID: 23141539; PMCID: 3496186.
35. Franken P, Chollet D, Tafti M. The homeostatic regulation of sleep need is under genetic control. JNeurosci. 2001;21(8):2610-21. PubMed PMID: 257.
36. Borbely AA, Daan S, Wirz-Justice A, Deboer T. The two-process model of sleep regulation: a reappraisal. J Sleep Res. 2016;25(2):131-43. doi: 10.1111/jsr.12371. PubMed PMID: 26762182.
37. Porkka-Heiskanen T, Strecker RE, Thakkar M, Bjorkum AA, Greene RW, McCarley RW. Adenosine: a mediator of the sleep-inducing effects of prolonged wakefulness. Science. 1997;276(5316):1265-8. doi: 10.1126/science.276.5316.1265. PubMed PMID: 9157887; PMCID: PMC3599777.
38. Brambilla D, Chapman D, Greene R. Adenosine mediation of presynaptic feedback inhibition of glutamate release. Neuron. 2005;46(2):275-83. Epub 2005/04/26. doi: 10.1016/j.neuron.2005.03.016. PubMed PMID: 15848805.

39. Greene RW, Bjorness TE, Suzuki A. The adenosine-mediated, neuronal-glial, homeostatic sleep response. Current opinion in neurobiology. 2017;44:236-42. doi: 10.1016/j.conb.2017.05.015. PubMed PMID: 28633050; PMCID: PMC5523826.
40. Bjorness TE, Dale N, Mettlach G, Sonneborn A, Sahin B, Fienberg AA, Yanagisawa M, Bibb JA, Greene RW. An Adenosine-Mediated Glial-Neuronal Circuit for Homeostatic Sleep. The Journal of neuroscience : the official journal of the Society for Neuroscience. 2016;36(13):3709-21. doi: 10.1523/JNEUROSCI.3906-15.2016. PubMed PMID: 27030757; PMCID: PMC4812131.
41. Myme CI, Sugino K, Turrigiano GG, Nelson SB. The NMDA-to-AMPA ratio at synapses onto layer 2/3 pyramidal neurons is conserved across prefrontal and visual cortices. Journal of neurophysiology. 2003;90(2):771-9. Epub 20030402. doi: 10.1152/jn.00070.2003. PubMed PMID: 12672778.
42. Zheng GX, Terry JM, Belgrader P, Ryvkin P, Bent ZW, Wilson R, Ziraldo SB, Wheeler TD, McDermott GP, Zhu J, Gregory MT, Shuga J, Montesclaros L, Underwood JG, Masquelier DA, Nishimura SY, Schnall-Levin M, Wyatt PW, Hindson CM, Bharadwaj R, Wong A, Ness KD, Beppu LW, Deeg HJ, McFarland C, Loeb KR, Valente WJ, Ericson NG, Stevens EA, Radich JP, Mikkelsen TS, Hindson BJ, Bielas JH. Massively parallel digital transcriptional profiling of single cells. Nat Commun. 2017;8:14049. Epub 20170116. doi: 10.1038/ncomms14049. PubMed PMID: 28091601; PMCID: PMC5241818.
43. Caglayan E, Liu Y, Konopka G. Neuronal ambient RNA contamination causes misinterpreted and masked cell types in brain single-nuclei datasets. Neuron. 2022;110(24):4043-56 e5. Epub 20221013. doi: 10.1016/j.neuron.2022.09.010. PubMed PMID: 36240767; PMCID: PMC9789184.

Acknowledgements
Funding support was provided by:
National Institute of Neurological Disorders and Stroke NS103422 to Robert W Greene
National Institute on Deafness and Other Communication Disorders DC014702 to Genevieve Konopka
James S. McDonnell Foundation 220020467 to Genevieve Konopka
International Institute for Integrative Sleep medicine to Kaspar Vogt. His research was also supported by AMED under Grant Number JP21zf0127005.